

# Assembly and structure of $\alpha$ -helical peptide films on hydrophobic fluorocarbon surfaces

Tobias Weidner and Newton T. Samuel<sup>a)</sup>

*Department of Bioengineering and Department of Chemical Engineering, National ESCA and Surface Analysis Center for Biomedical Problems, University of Washington, Seattle, Washington 98195*

Keith McCrea

*The Polymer Technology Group, Berkeley, California 94710*

Lara J. Gamble

*Department of Bioengineering and Department of Chemical Engineering, National ESCA and Surface Analysis Center for Biomedical Problems, University of Washington, Seattle, Washington 98195*

Robert S. Ward

*The Polymer Technology Group, Berkeley, California 94710*

David G. Castner<sup>b)</sup>

*Department of Bioengineering and Department of Chemical Engineering, National ESCA and Surface Analysis Center for Biomedical Problems, University of Washington, Seattle, Washington 98195*

(Received 31 December 2009; accepted 16 January 2010; published 3 March 2010)

The structure, orientation, and formation of amphiphilic  $\alpha$ -helix model peptide films on fluorocarbon surfaces has been monitored with sum frequency generation (SFG) vibrational spectroscopy, near-edge x-ray absorption fine structure (NEXAFS) spectroscopy, and x-ray photoelectron spectroscopy (XPS). The  $\alpha$ -helix peptide is a 14-mer of hydrophilic lysine and hydrophobic leucine residues with a hydrophobic periodicity of 3.5. This periodicity yields a rigid amphiphilic peptide with leucine and lysine side chains located on opposite sides. XPS composition analysis confirms the formation of a peptide film that covers about 75% of the surface. NEXAFS data are consistent with chemically intact adsorption of the peptides. A weak linear dichroism of the amide  $\pi^*$  is likely due to the broad distribution of amide bond orientations inherent to the  $\alpha$ -helical secondary structure. SFG spectra exhibit strong peaks near 2865 and 2935  $\text{cm}^{-1}$  related to aligned leucine side chains interacting with the hydrophobic surface. Water modes near 3200 and 3400  $\text{cm}^{-1}$  indicate ordering of water molecules in the adsorbed-peptide fluorocarbon surface interfacial region. Amide I peaks observed near 1655  $\text{cm}^{-1}$  confirm that the secondary structure is preserved in the adsorbed peptide. A kinetic study of the film formation process using XPS and SFG showed rapid adsorption of the peptides followed by a longer assembly process. Peptide SFG spectra taken at the air-buffer interface showed features related to well-ordered peptide films. Moving samples through the buffer surface led to the transfer of ordered peptide films onto the substrates. © 2010 American Vacuum Society. [DOI: 10.1116/1.3317116]

## I. INTRODUCTION

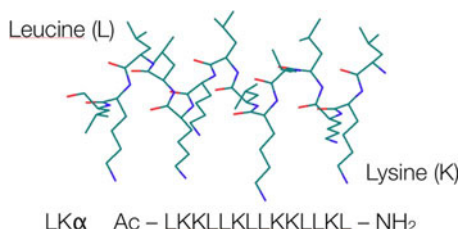
Understanding protein adsorption to interfaces at the molecular level is important for the development of surface coatings with specifically tailored biophysical properties.<sup>1</sup> Modification of surfaces is a key element in fields such as biomedical coatings, antifouling surfaces, and biosensors.<sup>2,3</sup> Protein films adsorbed onto artificial biointerfaces play a central role in these technologies and therefore structural details (chemical composition, orientation, secondary structure, etc.) of these films are of great interest.<sup>4–6</sup> Since proteins at interfaces are complex systems, it is useful to first investigate well-defined, model systems to develop standards for the analysis of biointerfaces.<sup>7</sup> In this context, custom-designed synthetic peptides of well-defined composition and second-

ary structure provide an opportunity to identify basic principles of protein adsorption. Amphiphilic model peptides made up of hydrophobic leucine (L) and hydrophilic lysine (K) side chains have been successfully used as model systems. Design parameters for synthesizing these peptides with the hydrophobic side chains on one side and the hydrophilic side chains on the other side have been described previously.<sup>8</sup>

Model LK peptides have been studied in solution and at the air/water interface for more than a decade,<sup>8–12</sup> but until recent years there have only been a few studies on solid surfaces.<sup>13,14</sup> Recently, LK adsorption has been investigated on a limited number of surfaces. Sum frequency generation (SFG) spectroscopy has proven to be a powerful technique for directly probing the structure of peptide films at the solid-liquid interface. In particular, studies of LK peptides on hydrophilic quartz surfaces,<sup>15,16</sup> hydrophobic polystyrene films,<sup>17,18</sup> and self-assembled monolayers<sup>18,19</sup> have revealed

<sup>a)</sup>Present address: CIBA VISION Corp., Duluth, GA 30097.

<sup>b)</sup>Author to whom correspondence should be addressed; electronic mail: castner@nb.engr.washington.edu



SCHEME 1. (Color online) Drawing of the synthetic LK $\alpha$ 14 peptide used in this study. This rigid  $\alpha$ -helical peptide has the hydrophilic lysine and the hydrophobic leucine residues on opposite sides.

some basic principles of the peptide orientation and binding chemistry. The effect of surface hydrophobicity, solvent ionic strength, and number of amino acids has also been studied.<sup>20,21</sup> The interaction of peptides with hydrophobic surfaces is of particular technological interest because a large number of biomaterials are hydrophobic and can potentially be functionalized with amphiphilic peptides.<sup>22–28</sup>

SFG can follow the *in situ* assembly of ordered layers with molecular level detail, and thus complements techniques sensitive to mass uptake on surfaces, such as quartz crystal microbalance<sup>29</sup> and surface plasmon resonance.<sup>30</sup> However, only a few *in situ*, real-time SFG experiments have been done to investigate the formation kinetics of protein films.<sup>16,31,32</sup> York *et al.*<sup>33</sup> published a preliminary kinetic study for LK peptides on polystyrene and SiO<sub>2</sub> in the CH and NH stretching ranges. Here we report an *in situ*, real-time kinetic study of the assembly of LK peptides onto hydrophobic fluorocarbon films where the important side chain related resonances (CH, NH) and backbone modes for peptide ordering are followed. Most importantly, we complement the SFG analysis with near-edge x-ray absorption fine structure (NEXAFS) spectra and kinetic x-ray photoelectron spectroscopy (XPS) data. In addition, we investigated ordered peptide layers at the air-buffer interface and the consequences of this layer for film preparation. The interaction of peptides with fluorocarbon films prepared by radio frequency glow discharge (RFGD) deposition of a hexafluoropropylene precursor is of technological and fundamental interest for many biomaterials applications.

The model peptide used here is a 14-mer  $\alpha$ -helix of hydrophilic lysine (K) and hydrophobic leucine (L) residues with a hydrophobic periodicity of 3.5 (LK $\alpha$ 14) (see Scheme 1). In addition to kinetic studies, a detailed *in situ* structural characterization of the prepared peptide films was done with SFG vibrational spectroscopy. The structural SFG experiments were complemented with *ex situ* NEXAFS and XPS studies.

## II. EXPERIMENTAL DETAILS

### A. Peptide synthesis

Amino acids used to synthesize the LK $\alpha$ 14 peptides in this study were Fmoc-Leu-OH and Fmoc-Lys(Boc)-OH (Novabiochem). The peptides were synthesized on a PS3

solid-state peptide synthesizer (Rainin) on a Leu-Wang resin (Novabiochem).

O-(benzotriazole-*N,N,N',N'*-tetramethyluronium hexafluorophosphate (Advanced ChemTech) was used as an activator, and the *N*-termini of the resin-bound peptides were capped following synthesis by acetylation with about 3 ml of acetic acid. Peptides were cleaved from the resin, dried by overnight lyophilization and their purity was checked using mass spectrometry following the procedures outlined by Long *et al.*<sup>34</sup> The final peptide sequence was Ac-LKKLLKLLKLLKL-OH.

### B. Radio frequency glow charge deposition

The fluorocarbon films were deposited from a hexafluoropropylene (HFP) RFGD using a home-built, inductively coupled rf reactor<sup>35</sup> described in detail elsewhere.<sup>36</sup> Cleaned CaF<sub>2</sub> substrates for SFG analysis were placed in the glow region of the reactor. They were initially etched in an argon pressure of 150 mTorr for 5 min at an input power of 40 W. A fluorocarbon film was then deposited onto the windows using an input power of 80 W for 1 min followed by a 4 min deposition with an input power of 20 W. The fluorocarbon films were quenched for 5 min under flowing HFP monomer with the radio frequency power turned off. The RFGD-deposited films were thin enough to avoid any significant attenuation of the laser beams used in the SFG experiments. Cleaned silicon pieces (Silicon Valley Microelectronics, Inc.) placed near the windows were also coated. These coated silicon pieces were then analyzed by XPS to determine the surface elemental composition of the fluorocarbon films.

### C. Peptide adsorption

Phosphate buffered saline (PBS) (pH=7.4) was obtained from FischerBiotech. The samples for XPS and NEXAFS analysis were prepared by placing 1 × 1 cm<sup>2</sup> pieces of the fluorocarbon coated silicon in 20  $\mu$ g/ml of the LK $\alpha$ 14 peptide solution in PBS (avoiding the air-water interface). The adsorption was done for 2 h in 1.5 ml polystyrene cups. The samples were then washed with de-ionized water by dilution displacement, blown dry with nitrogen, and then stored in plastic containers under inert gas until characterization with XPS or NEXAFS spectroscopy.

### D. X-ray photoelectron spectroscopy

All XPS data were acquired on a Surface Science Instruments X-probe spectrometer. This instrument has a monochromatized Al K $\alpha$  x-ray source and a low energy electron flood gun for charge neutralization. X-ray spot size for these acquisitions was  $\sim$ 800  $\mu$ m. Base pressure in the analytical chamber during spectral acquisition was better than 5 × 10<sup>−9</sup> Torr. The analyzer pass energies used to acquire the survey spectra (composition) and high-resolution C 1s spectra were 150 and 50 eV, respectively. The take-off angle (the angle between the sample normal and the input axis of the analyzer lens) was 55°.

The Service Physics ESCAVB Graphics Viewer program was used to determine peak areas, to calculate the elemental compositions from peak areas, and to fit the high-resolution spectra. The surface composition data for the peptide-covered samples represent the average over two different samples and two spots per sample. The data for the control samples represent the average over eight different samples from several different depositions of the plasma polymer.

### E. Near-edge x-ray absorption fine structure spectroscopy

The NEXAFS experiments were performed at the National Synchrotron Light Source (NSLS) U7-A beamline at Brookhaven National Laboratory. The beamline uses an  $\sim 85\%$  polarized beam and a monochromator with 600 l/mm grating producing a full width at half maximum energy resolution of  $\sim 0.15$  eV at the carbon  $K$ -edge. The monochromator energy scale for the oxygen edge was calibrated using the absorption peaks in the  $I_o$  grid spectra. These peaks were first calibrated by setting the  $C1s \rightarrow \pi^*$  transition in the graphite carbon  $K$ -edge NEXAFS spectrum to 285.35 eV. The nitrogen edge was calibrated to the intense  $\pi^*$  amide feature of poly(glycine) at 401.5 eV. The NEXAFS spectra were normalized with the signal from an *in situ* gold coated 90% transmission grid placed in the path of the x rays. Partial electron yield was monitored using a bias voltage of  $-280$  V for the nitrogen  $K$ -edge and  $-390$  V for the oxygen  $K$ -edge. The pre-edge was subtracted from the spectra using a linear background and the spectra were normalized to a unity absorption jump height.

### F. Sum frequency generation vibrational spectroscopy

The SFG spectra were obtained by overlapping visible and tunable IR laser pulses (25 ps) in time and space at incidence angles of  $60^\circ$  and  $54^\circ$ , respectively. The visible beam with a wavelength of 532 nm was delivered by an EKSPLA Nd:YAG (yttrium aluminum garnet) laser operating at 10 Hz, which was also used to pump a LaserVision optical parametric generation/amplification and difference frequency unit based on potassium titanium oxide phosphate and either  $\text{AgGaS}_2$  ( $1500\text{--}2000\text{ cm}^{-1}$ ) or potassium titanyl arsenate crystals ( $2000\text{--}4000\text{ cm}^{-1}$ ) to generate tunable IR laser radiation from 1500 to  $4000\text{ cm}^{-1}$ . Both beams were unfocused and had a diameter of approximately 3 mm at the sample. The energy for both beams was 160  $\mu\text{J}$  per pulse. The SFG signal generated at the sample was then analyzed by filters and a monochromator, detected with a gated photomultiplier tube, and stored in a computer. The spectra were collected with 400 shots per data point in  $1\text{--}4\text{ cm}^{-1}$  increments. All spectra were recorded in the *ssp* (sum, visible, and infrared) polarization combination.

## III. RESULTS

### A. Peptide film characterization

XPS elemental analysis was used to verify that LK $\alpha$ 14 forms stable films on the fluorocarbon (FC) surfaces. Table I

TABLE I. XPS determined elemental compositions of the HFP RFGD FC surface before and after adsorption of the LK $\alpha$ 14 peptide. The adsorption was done for 2 h from a 20  $\mu\text{g}/\text{ml}$  peptide solution in PBS.

Sample	Atomic percentage			
	C 1s	N 1s	O 1s	F 1s
FC control surface	$39.4 \pm 2.5$	$0.1 \pm 0.1$	$0.4 \pm 0.2$	$60.1 \pm 2.6$
LK $\alpha$ 14 peptide film	$52.1 \pm 1.8$	$4.2 \pm 0.4$	$5.7 \pm 0.2$	$38.0 \pm 1.6$

summarizes the chemical composition of the FC substrates with and without air-dried peptide films. For the FC films only carbon and fluorine with traces of oxygen and nitrogen were detected. This surface elemental composition is in good agreement with previously published data.<sup>37</sup> Compared to the untreated FC substrates, the peptide-covered FC surfaces exhibit a decreased fluorine signal and increased carbon signal due to attenuation of the substrate fluorine signal and addition of carbon from the adsorbed peptide layer. As expected, the nitrogen and oxygen concentrations increased significantly with peptide adsorption. The overlayer model of Paynter<sup>38</sup> can be used to estimate the peptide coverage on the FC surface. The data used in this calculation were the XPS composition of the control FC surface from Table I, the theoretical peptide composition (70.5 at. % C, 11.3 at. % N, and 13.1 at. % O), a peptide monolayer thickness of 1.4 nm, and peptide overlayer density of 1.2  $\text{g}/\text{cm}^3$ .<sup>39</sup> Based on the 1.2  $\text{g}/\text{cm}^3$  density mean free paths of 32, 30, 28, and 26 Å were calculated for the C, N, O, and F 1s photoelectrons, respectively.<sup>40</sup> Further details about LK peptide overlayer calculations have been described elsewhere.<sup>39</sup> Comparing these calculations for a theoretical LK $\alpha$ 14/FC sample to the experimental results indicated that the adsorption conditions used to prepare the XPS and NEXAFS samples produced a peptide coverage of approximately 75% of a monolayer.

NEXAFS spectra provide complementary information about the electronic structure of the LK $\alpha$ 14 films, sampling the electronic structure of the unoccupied molecular orbitals of the peptides.<sup>41</sup> The nitrogen  $K$ -edge spectra recorded at  $90^\circ$  and  $20^\circ$  angles of x-ray incidence are shown in Fig. 1 (left panel). The spectra exhibit a sharp resonance at  $\approx 401.5$  eV (amide  $\pi^*$  orbital), as well as two broader resonances at  $\approx 406.4$  eV (N–H  $\sigma^*$  orbital) and  $\approx 413.0$  eV (N–C  $\sigma^*$  orbital).<sup>42–44</sup> The weak pre-edge feature near 398.8 eV can either be assigned to positively charged amine groups on the lysine side chains<sup>45,46</sup> or traces of nitrogen contaminants in the underlying FC film.

NEXAFS spectra also provide valuable information about the orientation and order of the film constituents since the cross section of the NEXAFS process depends on the orientation of the incoming photon electric field vector with respect to the transition dipole moment (TDM) of the probed molecular orbital.<sup>41</sup> This linear dichroism is typically monitored by examining the difference between spectra acquired at normal ( $90^\circ$ ) and grazing ( $20^\circ$ ) photon incidences. The observed difference spectrum in Fig. 1 exhibits a weak but discernible negative linear dichroism for the LK $\alpha$ 14 amide

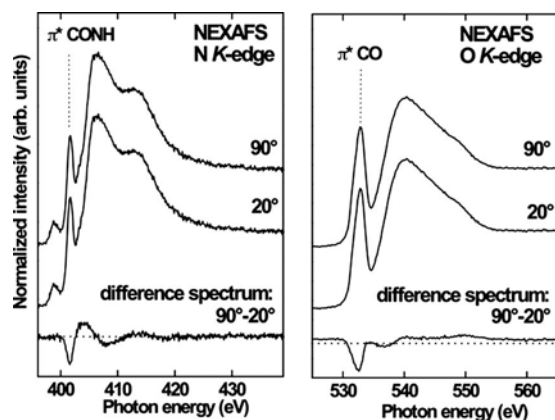


FIG. 1. Nitrogen and oxygen  $K$ -edge NEXAFS spectra of LK $\alpha$ 14 peptides adsorbed onto a fluorocarbon surface acquired at x-ray incidence angles of 90° and 20°, along with the difference between the 90° and the 20° spectra. Characteristic amide and carbonyl absorption resonances are indicated.

resonance. The weak dichroism can be explained by the intrinsically broad distribution of amide bond orientations in helical secondary structures.<sup>19</sup> However, the amide bond has a bent shape and in helical peptide structures it can be separated into two components: a radial component with an almost uniform orientation distribution (not leading to any NEXAFS dichroism) and a component along the backbone axis. The negative sign of the dichroism shows that the amide bond is oriented nominally parallel to the surface since the TDM of the latter amide  $\pi^*$  component is oriented perpendicular to the plane of the peptide (CONH) bond.<sup>41</sup> This has also been observed for LK $\alpha$ 14 peptides on self-assembled monolayers.<sup>19</sup>

This orientational analysis is further supported by O  $K$ -edge NEXAFS spectra for 90° and 20° incident x-ray angles displayed in Fig. 1 (right panel). The spectra consist of a sharp pre-edge feature near 531.8 eV related to transitions into the CO  $\pi^*$  orbital along with two broad  $\sigma^*$  resonances at higher photon energies.<sup>47</sup> The negative dichroism of the CO  $\pi^*$  resonance in the difference spectrum confirms that the CO bond is nominally oriented parallel to the interface.

The XPS and NEXAFS data are consistent with the LK $\alpha$ 14 peptides forming stable, well-defined films on FC substrates. To complement the XPS and NEXAFS data acquired from air-dried films under ultrahigh vacuum conditions, we analyzed the peptide films in buffer using SFG spectroscopy. Figure 2 shows typical SFG spectra of the peptides recorded at the buffer-fluorocarbon interface. Note that while peptides were also present in the surrounding buffer solution during the measurements, the spectrum is only representative of ordered adsorbed peptides on the surface because of the interface specificity and selection rules of the SFG technique.<sup>48,49</sup> The upper panel of Fig. 2 shows OH stretching modes near 3200 and 3400  $\text{cm}^{-1}$  related to tetrahedrally coordinated (“ice-like”) and hydrogen-bonded (“liquid-like”) water, respectively.<sup>50–52</sup> For LK peptides adsorbed onto hydrophobic surfaces, the presence of these water modes has been attributed to the interaction of hydro-

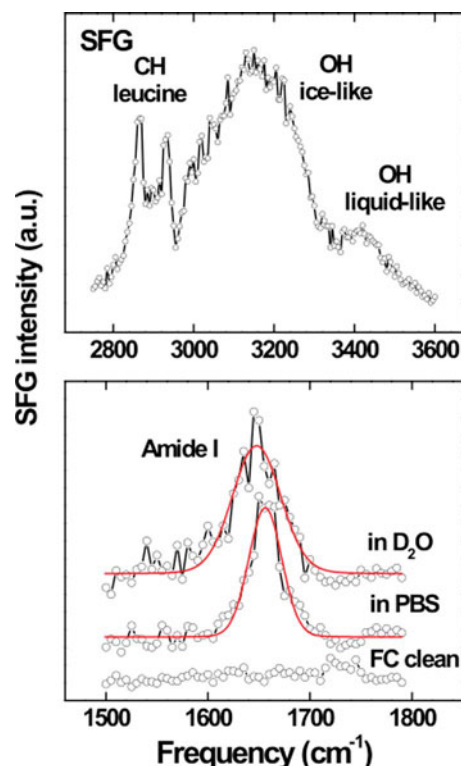


FIG. 2. (Color online) Upper panel: SFG spectrum of LK $\alpha$ 14 peptides adsorbed onto a fluorocarbon surface. The broad peaks near 3200 and 3400  $\text{cm}^{-1}$  are related to structured interfacial water molecules. The peaks near 2965 and 2930  $\text{cm}^{-1}$  are assigned to ordered leucine side chains. Lower panel: amide I SFG spectra of the same sample taken in PBS and after injection of deuterated water into the liquid cell. The peak centered at 1655  $\text{cm}^{-1}$  in PBS is characteristic of  $\alpha$ -helical secondary structures. The  $\sim 10$   $\text{cm}^{-1}$  redshift upon injection of deuterated water comes from H/D exchange at the nitrogen atoms in the peptide backbone.

philic lysine side chains with interfacial water molecules.<sup>15,20,21</sup> The CH stretching modes observed at 2865 and 2930  $\text{cm}^{-1}$  in the spectrum are commonly assigned to symmetric  $\text{CH}_3$  stretching modes and the  $\text{CH}_3$  Fermi resonance of the leucine side chain methyl groups, respectively.<sup>15,18,20,21,53,54</sup> These methyl related spectral features indicate the leucine side chains exhibit a significant degree of orientational order, most likely induced by interactions with the hydrophobic FC surface. Thus, the spectrum in the upper panel of Fig. 2 is consistent with the LK $\alpha$ 14 peptide oriented with the leucine side chains pointing toward the FC surface and the lysine side chains pointing away from the FC surface.

*In situ* amide I spectra of the adsorbed peptides are displayed in the lower panel of Fig. 2. The lower trace is recorded in PBS and exhibits a strong amide I signal near 1655  $\text{cm}^{-1}$  characteristic of an  $\alpha$ -helical secondary structure.<sup>55–57</sup> Upon replacing the PBS with deuterated water the amide I peak redshifts by  $\sim 10$   $\text{cm}^{-1}$ . This observation is consistent with the amide I redshift reported in literature for hydrogen-deuterium exchange at the nitrogen atoms in the peptide backbone.<sup>55</sup>

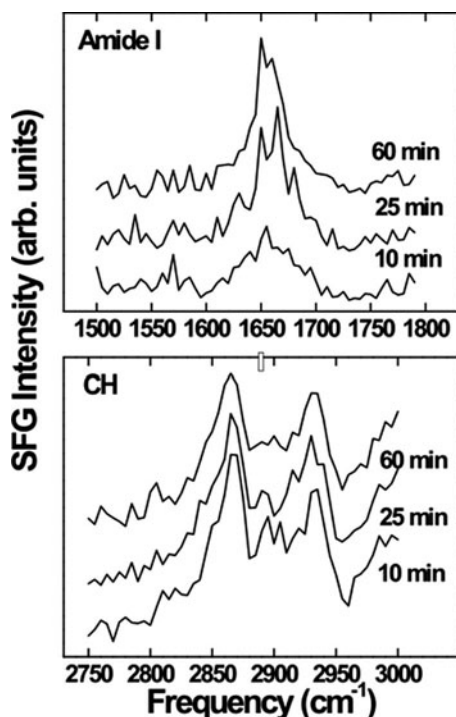


FIG. 3. SFG CH (lower panel) and amide I (upper panel) spectra of the LK $\alpha$ 14 peptides adsorbed onto fluorocarbon films after different adsorption times. While the amide I signal increases with exposure time, the CH spectra do not change with exposure time.

## B. Film formation

Using SFG we monitored *in situ* the LK $\alpha$ 14 peptide adsorption and film ordering process from a 20  $\mu$ g/ml PBS solution. Figure 3 shows quick scans of the amide I (upper panel) and CH spectral regions (lower panel) recorded after 10, 25, and 60 min of peptide solution exposure to the FC substrate. While the amide I peak near 1655  $\text{cm}^{-1}$  is still rather weak after 10 min and increases over time, we find that the leucine related CH stretches near 2869 and 2930  $\text{cm}^{-1}$  do not exhibit any noticeable variation with exposure time. The time course of the adsorption process was followed in more detail by simultaneously recording SFG signals at fixed IR frequencies while the FC substrate was exposed to the peptide solution. These kinetic measurements are shown in Fig. 4 for the amide I (upper panel) and CH stretching modes (lower panel). The arrows mark the starting point of the adsorption experiment when the peptide solution is injected into the cell. For the amide I analysis, the SFG intensities at 1655 and 1550  $\text{cm}^{-1}$  were recorded. The latter frequency was monitored as a control as no resonant mode is expected to be present at 1550  $\text{cm}^{-1}$ . Indeed no significant intensity changes at the control frequency were detected, but the amide I signal at 1655  $\text{cm}^{-1}$  did increase with peptide exposure for  $\sim 40$  min and then leveled off. Conversely, the leucine related resonances shown in the lower panel of Fig. 4 exhibited a steplike increase upon peptide injection. Since the SFG intensity is correlated with the order of interfacial moieties, we can conclude that the leucine side chains orient almost instantaneously, while the peptide backbones require

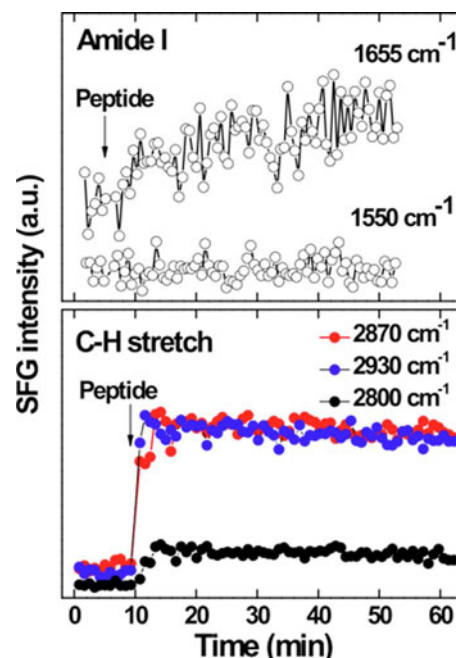


FIG. 4. (Color online) Real-time SFG intensities recorded during the adsorption of LK $\alpha$ 14 peptides onto a fluorocarbon surface. The intensities for characteristic resonance frequencies are shown along with intensities for frequencies where no resonances are expected (controls). The amide I signal (1655  $\text{cm}^{-1}$ ) increases with time, while the CH signals (2870 and 2930  $\text{cm}^{-1}$ ) show a steplike time behavior.

more time to assume their final orientation and arrangement. York *et al.*<sup>33</sup> observed significantly slower leucine ordering kinetics for LK $\alpha$ 14 on polystyrene. This suggests that the nature of the hydrophobic surface (FC versus polystyrene) plays a role in the LK $\alpha$ 14 adsorption process. The immediate increase in the leucine methyl group peaks on the FC surface indicates that the peptide adsorption process is rapid, but the gradual increase in the amide I peak indicates that rearrangement of the peptides occurs with adsorption time. The results from air-dried peptide films analyzed by XPS after different adsorption times in a 20  $\mu$ g/ml peptide solution support the SFG kinetic observations. XPS composition data for these films are summarized in Fig. 5. Increasing carbon, oxygen,

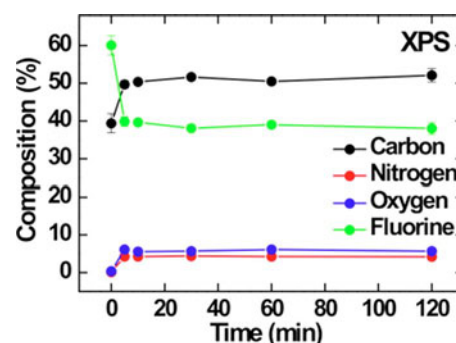


FIG. 5. (Color online) XPS determined elemental compositions of fluorocarbon surfaces after different LK $\alpha$ 14 peptide adsorption times. The decrease in fluorine concentration along with the increase of carbon, nitrogen, and oxygen concentration are characteristic of peptides adsorbing onto the fluorocarbon surface. The XPS data show a steplike adsorption behavior.

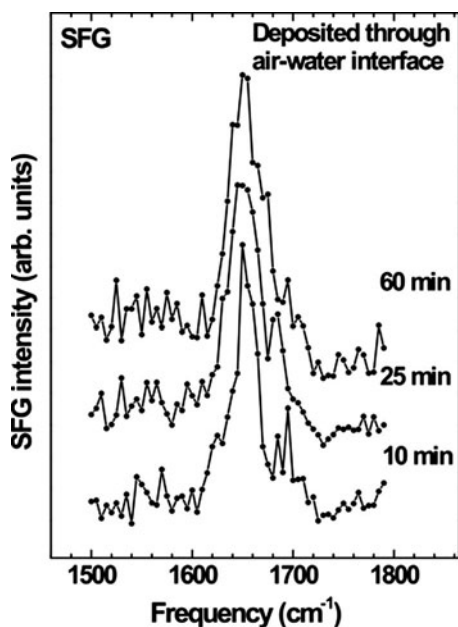


FIG. 6. SFG amide I spectra taken for different exposition times of a fluorocarbon substrate to the LK $\alpha$ 14 peptide solution after the sample was moved through the solution-air interface. There are no time dependent intensity variations detectable in the spectra.

and nitrogen concentrations along with a decreasing fluorine concentration are consistent with adsorption of peptides onto the FC surface. According to the XPS kinetic data the peptides reach saturation coverage within 5 min. This observation is similar to the ordering kinetics of the leucine side chains measured with SFG. This is not surprising since the LK $\alpha$ 14 peptide adsorption occurs via hydrophobic interaction between the leucine methyl groups and the FC substrate. This interaction, in turn, leads to ordering of the leucine chains.

In summary, the ordering of the leucine side chains, as seen from time dependent SFG spectra (Figs. 3 and 4, lower panel) and the increase in peptide coverage on the surface observed with XPS, follows similar kinetics. This again supports the hypothesis that the interaction of the leucine side chains with the surface is the main driving force for the LK14 peptide adsorption. Conversely, the amide signal related to the orientational order of the peptide backbone increases gradually over time. It samples the alignment process within the LK14 peptide layer and reveals that the lateral ordering within the film toward a well-defined layer occurs on the time scale of hours. Ordering of protein backbones on the same timescale has also been observed for fibrinogen on poly(ether urethane).<sup>58</sup>

A markedly different kinetic behavior is observed if the FC surface is moved through the air-peptide solution interface instead of avoiding the air-solution interface by injecting a concentrated peptide stock solution into the buffer-filled liquid cell as described above. SFG amide I spectra recorded at different exposure times after the FC substrate was moved through the air-peptide solution interface are shown in Fig. 6. Unlike the adsorption method that avoided

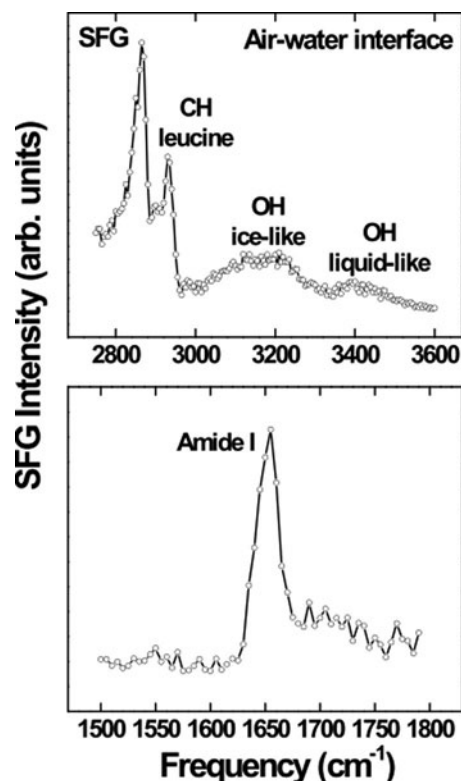


FIG. 7. Upper panel: SFG spectrum of LK $\alpha$ 14 peptides at the air-buffer interface. The broad peaks near 3200 and 3400  $\text{cm}^{-1}$  are related to structured water molecules. The peaks near 2965 and 2930  $\text{cm}^{-1}$  are assigned to ordered leucine side chains. Lower panel: amide I SFG spectra of the same sample. The peak centered at 1655  $\text{cm}^{-1}$  is characteristic of an  $\alpha$ -helical secondary structure.

the air-peptide solution interface, no significant time dependence of the amide I peak intensity was detected in this case. The amide I signal is already at its maximum intensity in the first spectrum taken after 10 min. This effect was further studied by examining the structure of LK14 peptides at the air-buffer interface with SFG. The SFG spectrum in the upper panel of Fig. 7 exhibits strong CH stretches related to the leucine side chains near 2865 and 2930  $\text{cm}^{-1}$  along with two broad OH related resonances near 3200 and 3400  $\text{cm}^{-1}$  related to tetrahedrally coordinated and hydrogen-bonded water, respectively.<sup>15,20,21,50–52</sup> As observed on the FC surface the lysine side chains likely interact with and order interfacial water molecules, while the hydrophobic leucine side chains point away from the water surface. This agrees very well with earlier structural studies of water surfaces where the air-water interface was described as hydrophobic.<sup>50</sup> The strong amide I peak observed near 1655  $\text{cm}^{-1}$  (Fig. 7, lower panel) shows the  $\alpha$ -helical secondary structure of the peptides is maintained at the air-solution interface.<sup>55–57</sup> It can be concluded that an ordered and aligned layer of LK $\alpha$ 14 peptides form at the air-buffer interface. We conclude that moving the substrate through the ordered peptide layer at the buffer surface transfers this film onto the substrate, similar to a Langmuir–Blodgett-type film deposition. The XPS analysis of this deposited film reveals that only a peptide monolayer is transferred onto the surface (data not shown), which makes

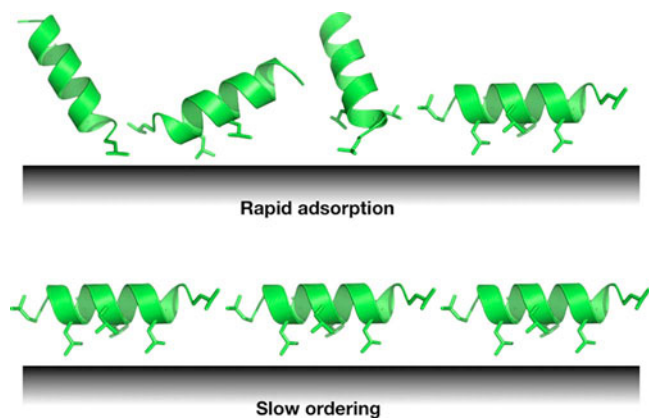


FIG. 8. (Color online) Schematic for the proposed two-step adsorption process: In the first step the peptides bind to the surface within minutes with their backbones mostly disordered. Some of the leucine side chains bind the peptides to the fluorocarbon surface via hydrophobic interactions, becoming ordered and detectable by SFG. In the second step, taking a period of hours, the peptide backbones align and an ordered monolayer is formed. A similar number of ordered leucine side chains are present throughout the backbone alignment step (the ordered side chains are shown as the ones pointing toward the surface). A small amount peptide desorption (<20% of the initially adsorbed peptide layer based on the XPS results) may occur during the rearrangement step as the peptide backbones become aligned.

it very likely that the original peptide film at the buffer-air interface is also comprised of only a single layer.

#### IV. SUMMARY

An investigation of the amphiphilic LK $\alpha$ 14 model peptide adsorption onto hydrophobic RFGD-deposited FC films has been performed by combining *in situ* (SFG) and *ex situ* characterization (XPS and NEXAFS) methods. On the FC substrate the peptide maintains its native  $\alpha$ -helical secondary structure and is bound via hydrophobic interactions between its leucine side chains and the FC surface. The lysine side chains point away from the interface and interact with the surrounding water molecules creating an interfacial layer of structured water. The peptides form well-ordered films with their backbones parallel to the surface. This occurs in a two-step process (see Fig. 8 for a proposed schematic): (i) The LK $\alpha$ 14 peptides first adsorb within a few minutes onto the FC surface with ordered leucine side chain methyl groups, but a mostly disordered peptide backbone. (ii) Then rearrangement over a period of tens of minutes occurs leading to a peptide layer with well-aligned peptide backbones. The number of ordered methyl groups does not change significantly during the ordering of the peptide backbone. LK $\alpha$ 14 peptides were also observed to form a well-ordered monolayer at the buffer-air interface. This film can be transferred to the fluorocarbon surface by moving the FC substrate through the air-buffer interface, depositing a well-aligned peptide film onto the FC substrate.

#### ACKNOWLEDGMENTS

Financial support by the National Institutes of Health under Grant Nos. GM-074511 and EB-002027 (NESAC/Bio) is gratefully acknowledged. T.W. thanks the Deutsche

Forschungsgemeinschaft for a research fellowship. The authors also thank Daniel Fischer and Cherno Jaye for their expert technical assistance with the NEXAFS experiments. NEXAFS studies were performed at the NSLS, Brookhaven National Laboratory, which was supported by the U.S. Department of Energy, Division of Materials Science and Division of Chemical Sciences.

<sup>1</sup>T. A. Horbett and J. L. Brash, *Proteins at Interfaces II: Fundamentals and Applications* (American Chemical Society, Washington D. C., 1995).

<sup>2</sup>B. D. Ratner, *Macromol. Symp.* **130**, 327 (1997).

<sup>3</sup>B. D. Ratner and S. J. Bryant, *Annu. Rev. Biomed. Eng.* **6**, 41 (2004).

<sup>4</sup>D. H. Fremont, M. Matsumura, E. A. Stura, P. A. Peterson, and I. A. Wilson, *Science* **257**, 919 (1992).

<sup>5</sup>C. J. Russell, T. E. Thorgeirsson, and Y. K. Shin, *Biochemistry* **35**, 9526 (1996).

<sup>6</sup>P. Krüger, M. Schälke, Z. Wang, R. H. Notter, R. A. Dluhy, and M. Losche, *Biophys. J.* **77**, 903 (1999).

<sup>7</sup>D. G. Castner and B. D. Ratner, *Surf. Sci.* **500**, 28 (2002).

<sup>8</sup>W. F. DeGrado and J. D. Lear, *J. Am. Chem. Soc.* **107**, 7684 (1985).

<sup>9</sup>A. Kerth, A. Erbe, M. Dathe, and A. Blume, *Biophys. J.* **86**, 3750 (2004).

<sup>10</sup>L. Beven, S. Castano, J. Dufourcq, A. Wieslander, and H. Wroblewski, *Eur. J. Biochem.* **270**, 2207 (2003).

<sup>11</sup>S. Castano, B. Desbat, M. Laguerre, and J. Dufourcq, *Biochim. Biophys. Acta* **1416**, 176 (1999).

<sup>12</sup>D. Dieudonné, A. Gericke, C. R. Flach, X. Jiang, R. S. Farid, and R. Mendelsohn, *J. Am. Chem. Soc.* **120**, 792 (1998).

<sup>13</sup>S. Stewart and P. M. Fredericks, *Spectrochim. Acta, Part A* **55**, 1615 (1999).

<sup>14</sup>T. M. Herne, A. M. Ahern, and R. L. Garrell, *Anal. Chim. Acta* **246**, 75 (1991).

<sup>15</sup>O. Mermut, D. C. Phillips, R. L. York, K. R. McCrea, R. S. Ward, and G. A. Somorjai, *J. Am. Chem. Soc.* **128**, 3598 (2006).

<sup>16</sup>N. T. Samuel, Ph.D. thesis, University of Washington, 2005.

<sup>17</sup>T. Weidner, N. F. Breen, G. P. Dobny, and D. G. Castner, *J. Phys. Chem. B* **113**, 15423 (2009).

<sup>18</sup>N. F. Breen, T. Weidner, K. Li, D. G. Castner, and G. P. Dobny, *J. Am. Chem. Soc.* **131**, 14148 (2009).

<sup>19</sup>T. Weidner, J. Apte, L. J. Gamble, and D. G. Castner, "Probing the Orientation and Conformation of  $\alpha$ -Helix and  $\beta$ -Strand Model Peptides on Self-Assembled Monolayers Using Sum Frequency Generation and NEXAFS Spectroscopy," *Langmuir* (in press).

<sup>20</sup>R. L. York, O. Mermut, D. C. Phillips, K. R. McCrea, R. S. Ward, and G. A. Somorjai, *J. Phys. Chem. C* **111**, 8866 (2007).

<sup>21</sup>D. C. Phillips, R. L. York, O. Mermut, K. R. McCrea, R. S. Ward, and G. A. Somorjai, *J. Phys. Chem. C* **111**, 255 (2007).

<sup>22</sup>P. D. Drumheller, D. L. Elbert, and J. A. Hubbell, *Biotechnol. Bioeng.* **43**, 772 (1994).

<sup>23</sup>K. P. Walluscheck, G. Steinhoff, S. Kelm, and A. Haverich, *Eur. J. Vasc. Endovasc. Surg.* **12**, 321 (1996).

<sup>24</sup>J. A. Neff, K. D. Caldwell, and P. A. Tresco, *J. Biomed. Mater. Res.* **40**, 511 (1998).

<sup>25</sup>T. Pakalns, K. L. Haverstick, G. B. Fields, J. B. McCarthy, D. L. Mooradian, and M. Tirrell, *Biomaterials* **20**, 2265 (1999).

<sup>26</sup>K. Bhadriraju and L. K. Hansen, *Biomaterials* **21**, 267 (2000).

<sup>27</sup>I. Elloumi, R. Kobayashi, H. Funabashi, M. Mie, and E. Kobatake, *Biomaterials* **27**, 3451 (2006).

<sup>28</sup>M. I. Janssen, M. B. M. van Leeuwen, K. Scholtmeijer, T. G. van Kooten, L. Dijkhuizen, and H. A. B. Wosten, *Biomaterials* **23**, 4847 (2002).

<sup>29</sup>M. Rodahl, F. Hook, A. Krozer, P. Brzezinski, and B. Kasemo, *Rev. Sci. Instrum.* **66**, 3924 (1995).

<sup>30</sup>L. S. Jung, J. S. Shumaker-Parry, C. T. Campbell, S. S. Yee, and M. H. Gelb, *J. Am. Chem. Soc.* **122**, 4177 (2000).

<sup>31</sup>X. Chen, M. L. Clarke, J. Wang, and Z. Chen, *Int. J. Mod. Phys. B* **19**, 511, 32691 (2005).

<sup>32</sup>J. Wang, X. Y. Chen, M. L. Clarke, and Z. Chen, *J. Phys. Chem. B* **110**, 513, 5017 (2006).

<sup>33</sup>R. L. York, W. K. Browne, P. L. Geissler, and G. A. Somorjai, *Isr. J. Chem.* **47**, 51 (2007).

<sup>34</sup>J. R. Long, N. Oyler, G. P. Dobny, and P. S. Stayton, *J. Am. Chem. Soc.*

- 124, 6297 (2002).
- <sup>35</sup>P. D. d'Agostino, *Treatment and Etching of Polymers* (Academic, San Diego, 1990).
- <sup>36</sup>M. C. Shen, Y. V. Pan, M. S. Wagner, K. D. Hauch, D. G. Castner, B. D. Ratner, and T. A. Horbett, *J. Biomater. Sci., Polym. Ed.* **12**, 961 (2001).
- <sup>37</sup>M. D. Garrison, R. Luginbuhl, R. M. Overney, and B. D. Ratner, *Thin Solid Films* **352**, 13 (1999).
- <sup>38</sup>R. W. Paynter, *Surf. Interface Anal.* **3**, 186 (1981).
- <sup>39</sup>J. S. Apte, G. Collier, R. A. Latour, L. J. Gamble and D. G. Castner, "XPS and ToF-SIMS Investigation of  $\alpha$ -Helical and  $\beta$ -Strand Peptide Adsorption onto SAMs," *Langmuir* (to be published).
- <sup>40</sup>M. P. Seah and W. A. Dench, *Surf. Interface Anal.* **1**, 2 (1979).
- <sup>41</sup>J. Stöhr, *NEXAFS Spectroscopy* (Springer, Berlin, 1992).
- <sup>42</sup>C. Cotton, A. Glidle, G. Beamson, and J. M. Cooper, *Langmuir* **14**, 5139 (1998).
- <sup>43</sup>Y. Zubavichus, M. Zharnikov, A. Schaporenko, and M. Grunze, *J. Electron Spectrosc. Relat. Phenom.* **134**, 25 (2004).
- <sup>44</sup>Y. Zubavichus, M. Zharnikov, A. Shaporenko, O. Fuchs, L. Weinhardt, C. Heske, E. Umbach, J. D. Denlinger, and M. Grunze, *J. Phys. Chem. A* **108**, 4557 (2004).
- <sup>45</sup>K. Ozawa, T. Hasegawa, K. Edamoto, K. Takahashi, and M. Kamada, *J. Phys. Chem. B* **106**, 9380 (2002).
- <sup>46</sup>J. E. Baio, T. Weidner, J. Brison, D. J. Graham, L. J. Gamble, and D. G. Castner, *J. Electron Spectrosc. Relat. Phenom.* **172**, 2 (2009).
- <sup>47</sup>M. L. Gordon, G. Cooper, C. Morin, T. Araki, C. C. Turci, K. Kaznatcheev, and A. P. Hitchcock, *J. Phys. Chem. A* **107**, 6144 (2003).
- <sup>48</sup>C. D. Bain, *J. Chem. Soc., Faraday Trans.* **91**, 1281 (1995).
- <sup>49</sup>P. Guyot-Sionnest, J. H. Hunt, and Y. R. Shen, *Phys. Rev. Lett.* **59**, 1597 (1987).
- <sup>50</sup>Q. Du, E. Freysz, and Y. R. Shen, *Science* **264**, 826 (1994).
- <sup>51</sup>N. Ji, V. Ostroverkhov, C. S. Tian, and Y. R. Shen, *Phys. Rev. Lett.* **100**, 096102 (2008).
- <sup>52</sup>C. S. Tian, N. Ji, G. A. Waychunas, and Y. R. Shen, *J. Am. Chem. Soc.* **130**, 13033 (2008).
- <sup>53</sup>M. Himmelhaus, F. Eisert, M. Buck, and M. Grunze, *J. Phys. Chem. B* **104**, 576 (2000).
- <sup>54</sup>M. R. Watry and G. L. Richmond, *J. Phys. Chem. B* **106**, 12517 (2002).
- <sup>55</sup>B. R. Singh, *Infrared Analysis of Peptides and Proteins* (American Chemical Society, Washington, D.C., 2000).
- <sup>56</sup>X. Chen, J. Wang, J. J. Sniadecki, M. A. Even, and Z. Chen, *Langmuir* **21**, 2662 (2005).
- <sup>57</sup>R. L. York, G. J. Holinga, D. R. Guyer, K. R. McCrea, R. S. Ward, and G. A. Somorjai, *Appl. Spectrosc.* **62**, 937 (2008).
- <sup>58</sup>M. L. Clarke, J. Wang, and Z. Chen, *J. Phys. Chem. B* **109**, 22027 (2005).